Electronic Supplementary Material (ESI) for RSC Advances.

ESIPT blocked CHEF based differential dual sensor for Zn^{2+} and Al^{3+}in pseudo-aqueous medium with intracellular bio-imaging applications and computational studies†

Rabiul Alam[a], Tarun Mistri[a] , Rahul Bhowmick[a], Atul Katarkar[b] ,Keya Chaudhuri[b]and Mahammad Ali*[a]

[a]Department of Chemistry, Jadavpur University, Kolkata 700 032, India, Fax: 91-33-2414-6223, E-mail: m_ali2062@yahoo.com,

[b]Molecular & Human Genetics Division , CSIR-Indian Institute of Chemical Biology , 4 Raja S.C. Mullick Road, Kolkata-700032, India

Supporting Information for Publication

Table of contents	
^{1}H NMR spectrum of H_3SAL-NH in DMSO-d_6, in Bruker 300 MHz instrument.	Figure S1
^{13}C NMR spectrum of H_3SAL-NH in DMSO-d_6, in Bruker 300 MHz instrument	Figure S2
Mass spectrum of H_3SAL-NH	Figure S3
Mass spectrum of Zn complex	FigureS3a
Mass spectrum of Al complex	Figure S3b
Absorption titration of with Al^{3+} in THF-H_2O (6:4, v/v) in HEPES buffer	FigureS4
Lifetime plot of ligand and ligand+ Zn^{2+} in T.H.F:H_2O (6:4 (V/V) in HEPES buffer	Figure S5
Lifetime plot of ligand and ligand+ Al^{3+} in T.H.F:H_2O(6:4 (V/V) in HEPES buffer.	FigureS6
UV-vis spectrum and Fluorescence excitation spectra of the ligand.	Figure S7
Spectra of Al^{3+} and after the addition of 1 equivalent Zn^{2+}	Figure S8
Reversibility plot of Zn^{2+} and Al^{3+} complex With Na_2H_2EDTA	Figure S9
LOD determination	Figure S10
FT-IR spectrum of H_3SAL-NH in KBr pellet.	Figure S11
FT-IR spectrum of Al Complex(complex 1)	Figure S11a
FT-IR spectrum of Zn Complex (complex 2)	Figure S11b
Frontier molecular orbitals involved in the UV-vis absorption of complex 2.	Figure S12
% cell viability study	Figure S13

^{1}H-NMR chemical shifts in ppm of selected H-atoms in DMSO-d_6	Table S1
Selective bond distance and bond angles of H_3SAL-NH, complex 1 and complex 2	Table S2
Selected parameters for the vertical excitation of H_3SAL-NH	Table S3
Main calculated optical transition for the complex 1	Table S4
Main calculated optical transition for the complex 2	Table S5
Emission band at lower wavelength (around 430 nm) and at higher Wavelength (above 520 nm) in various solvents.	Figure S14.
Titration with Al^{3+} in presence of 1equivalent H_2SAL-NH—Zn^{2+} and 1 equivalent Na_2H_2EDTA.	Figure S15

.

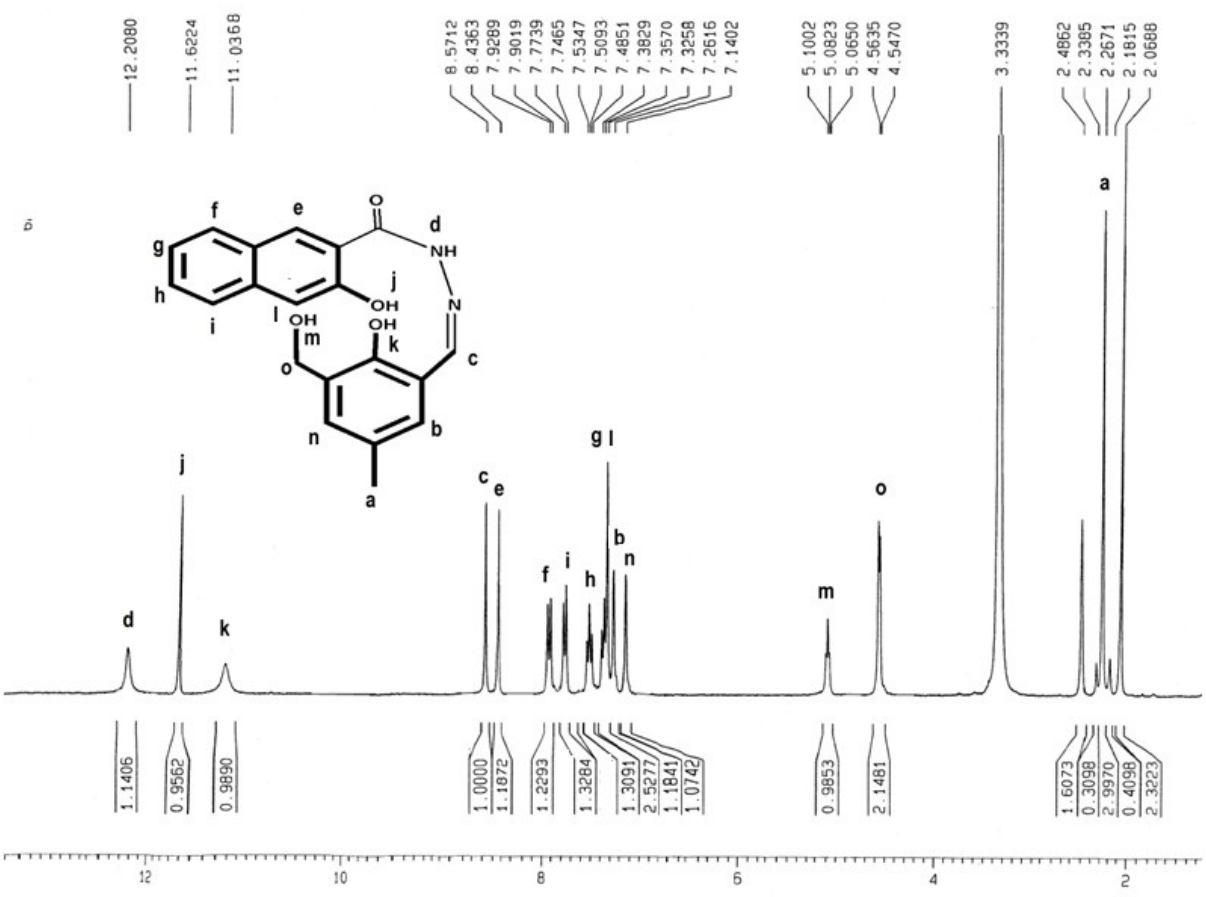

Figure S1. ^{1}H NMR spectrum of H_3SAL-NH in DMSO-d_6, in Bruker 300 MHz instrument**.**

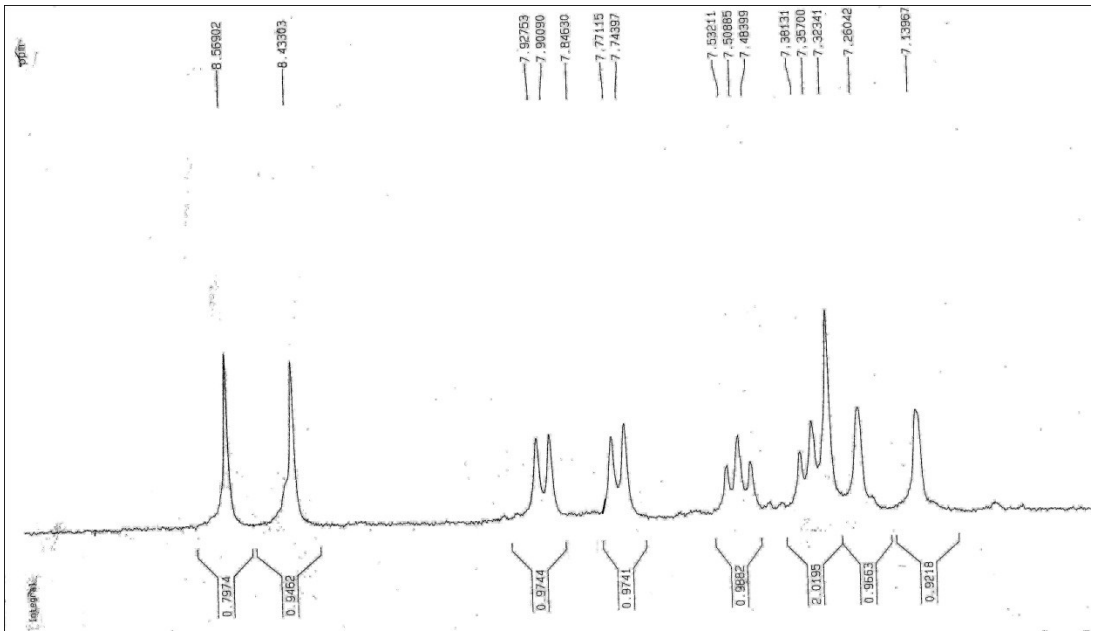

Figure S1. [1]H NMR spectrum of H_3SAL-NHin DMSO-d_6, in Bruker 300 MHz instrument.(Enlarge spectra 9-6 ppm

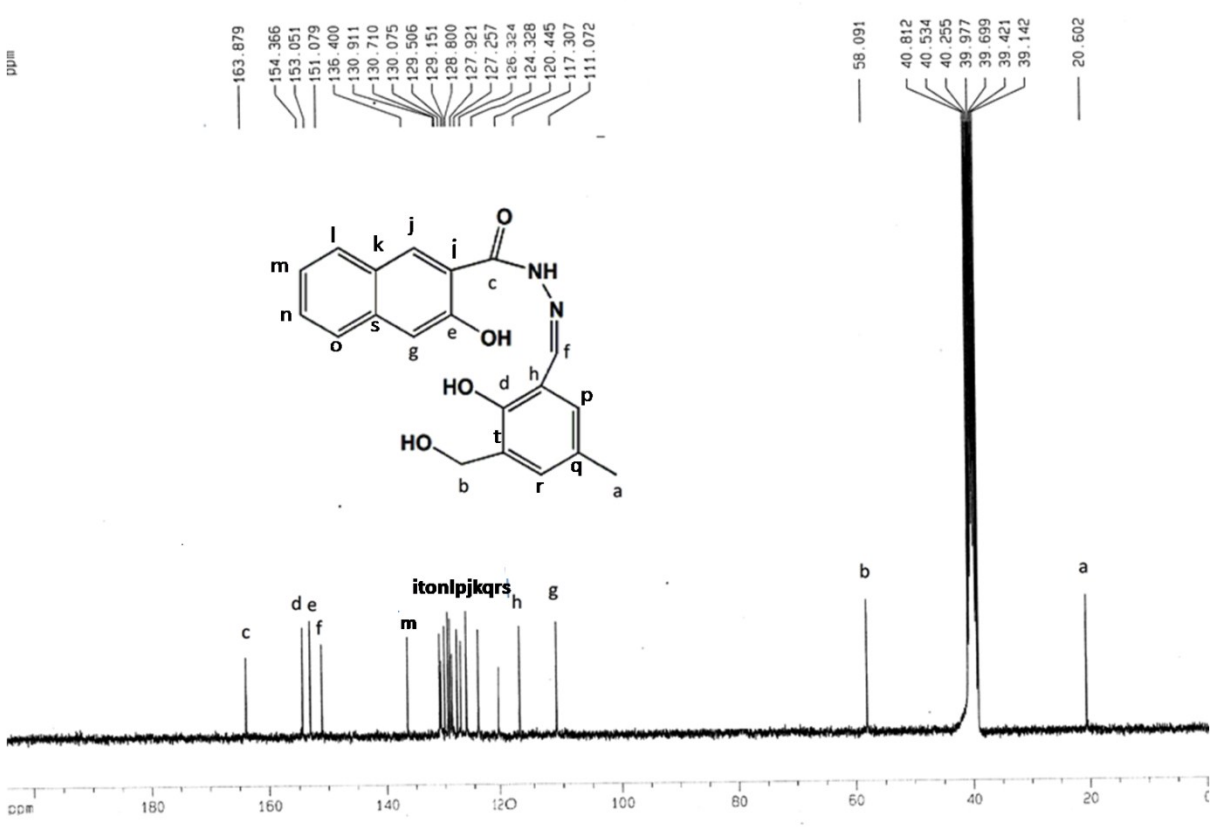

Figure S2. ^{13}C-NMR spectrum of H_3SAL-NH in DMSO-d_6, in Bruker 300 MHz instrument.

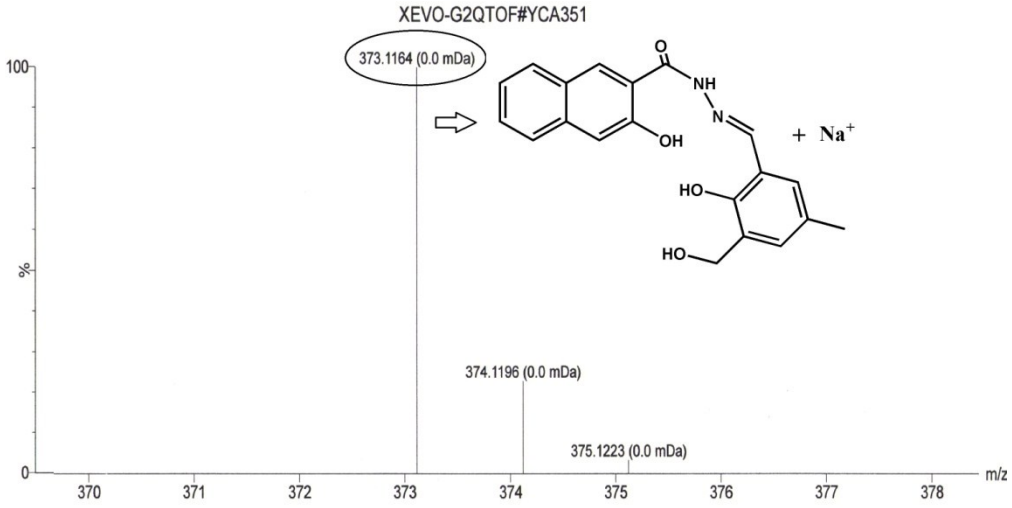

Figure S3. Mass spectrum of H_3SAL-NH in THF.

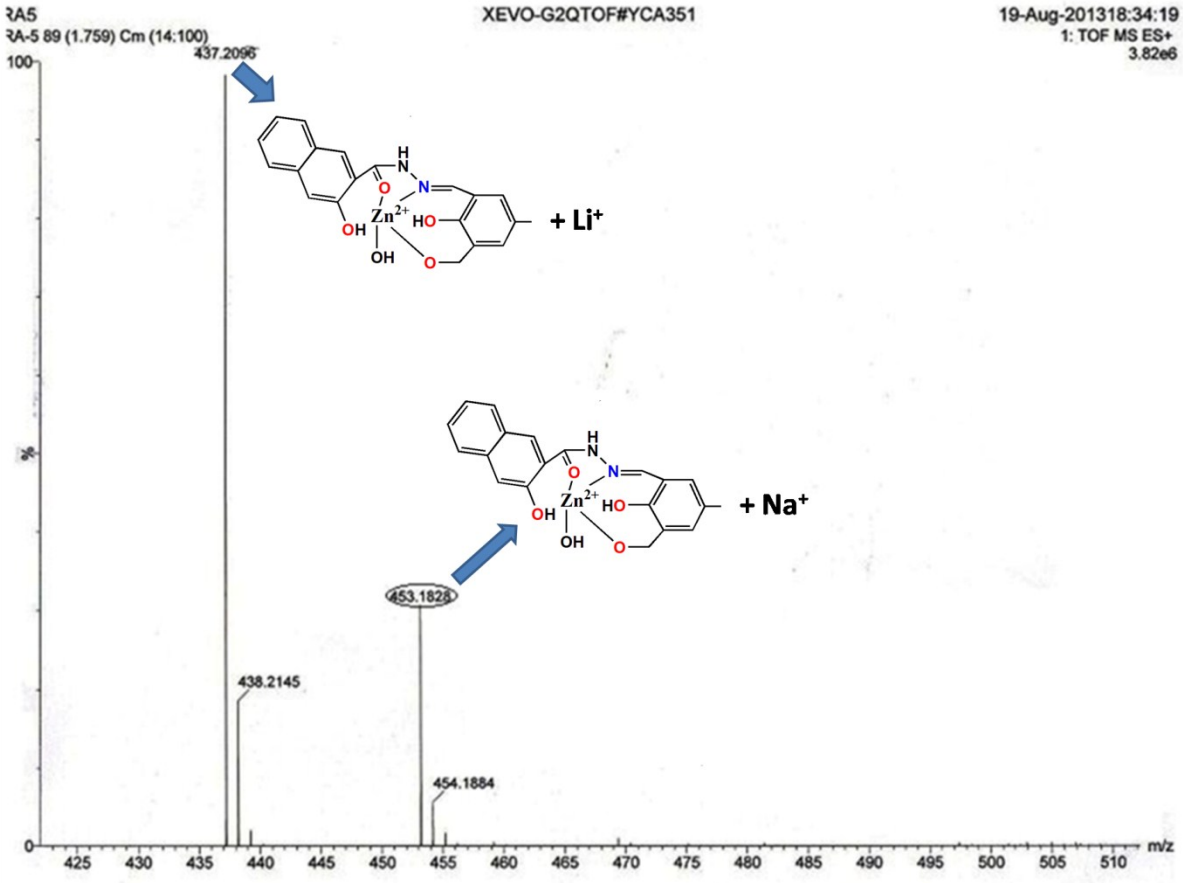

Figure S3a. Mass spectrum of H_2SAL-NH-Zn^{2+} in THF.

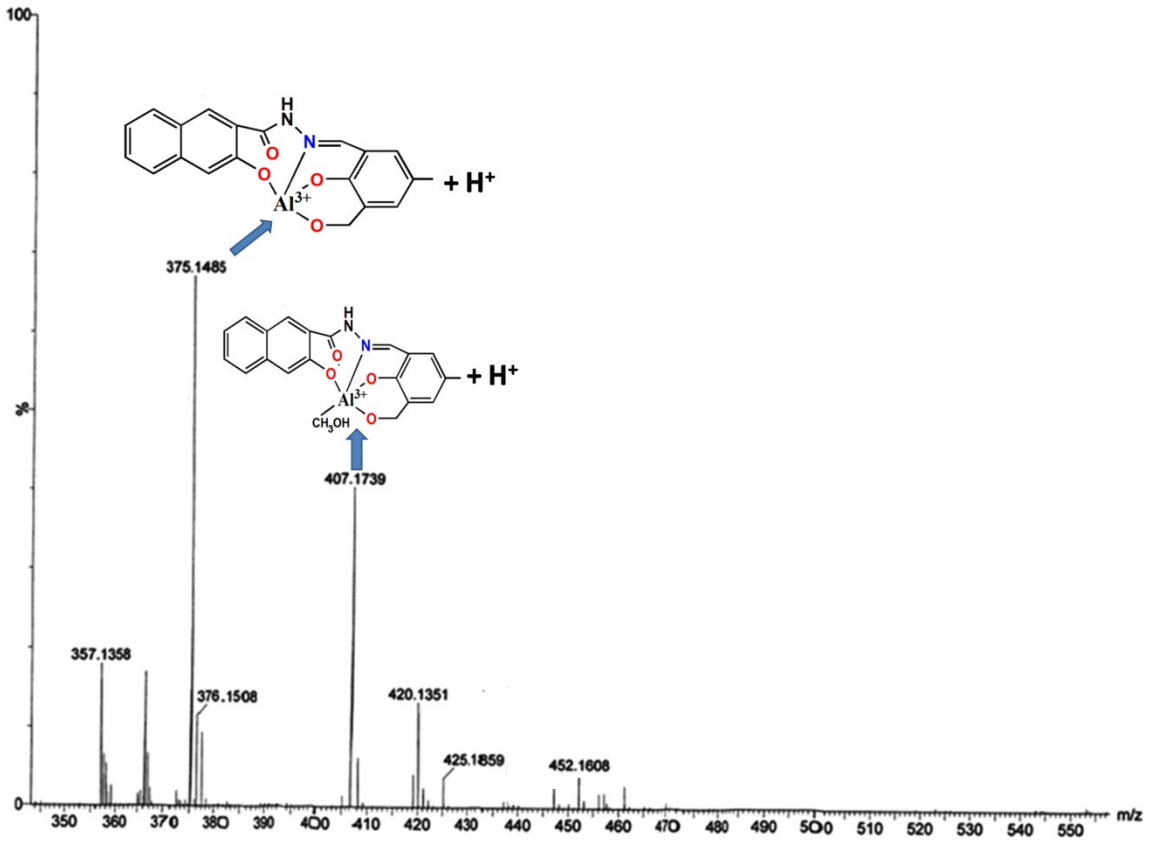

Figure S3b. Mass spectrum of SAL-NH-Al^{3+}in MeOH.

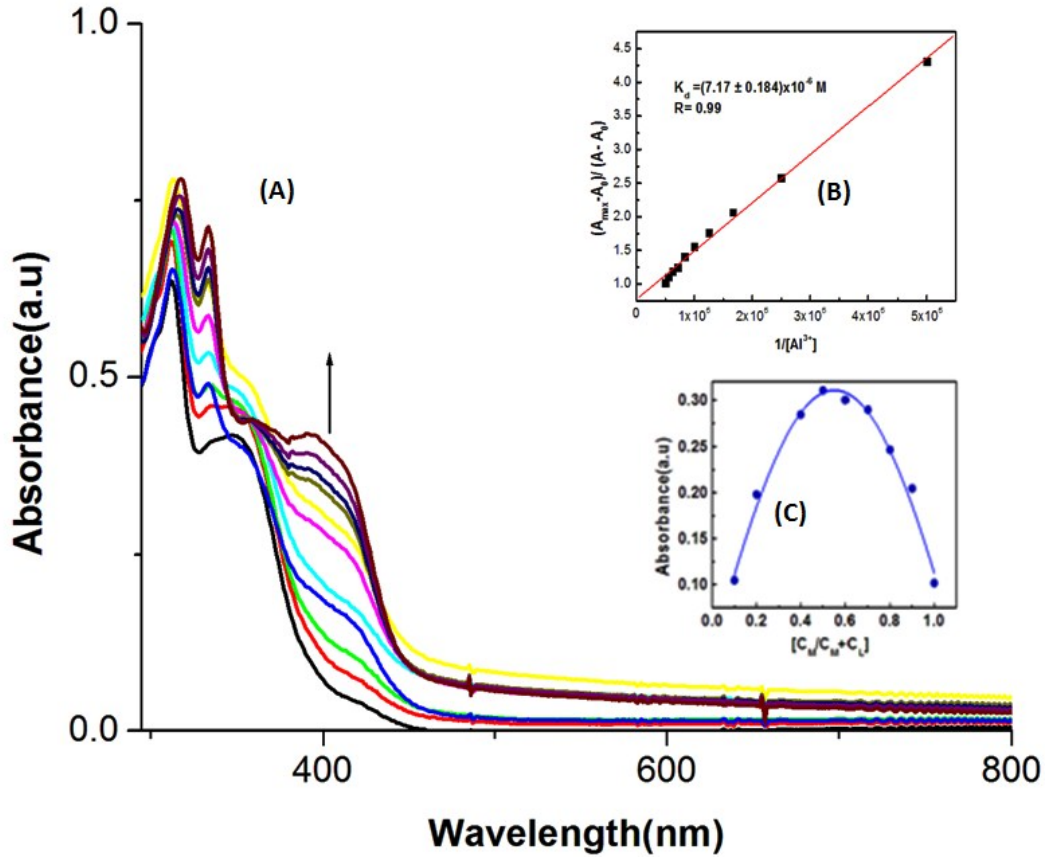

FigureS4. (A) Absorption titration of H_3SAL-NH with Al^{3+} in THF-H_2O (6:4, v/v) in HEPES buffer (1 mM) at pH 7.2; (B) Benesi-Hilderbrand plot; (C)JOB'S Plot.

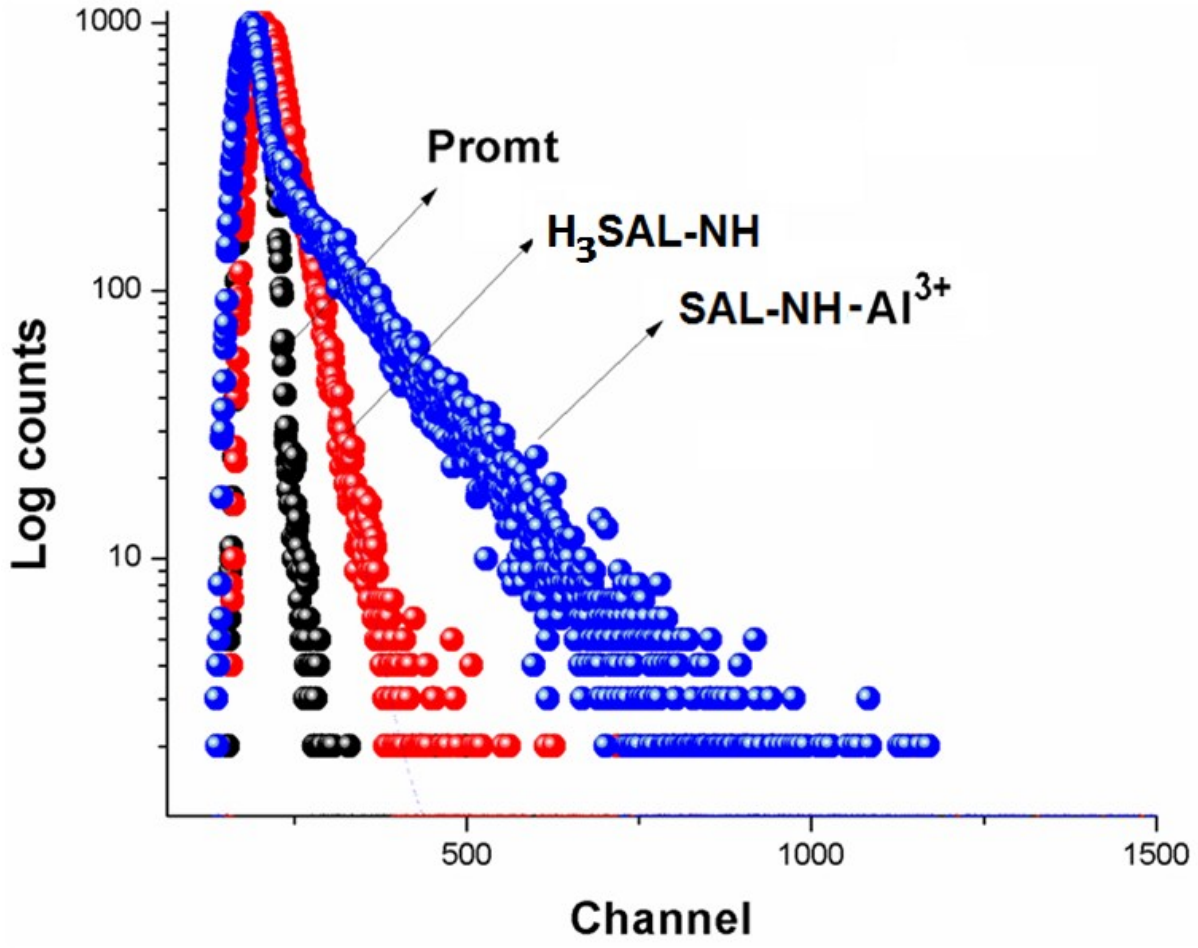

Figure S5. Lifetime plot of H_3SAL-NHandSAL-NH - Al^{3+} in T.H.F:H_2O (6:4 (V/V) in HEPES buffer.

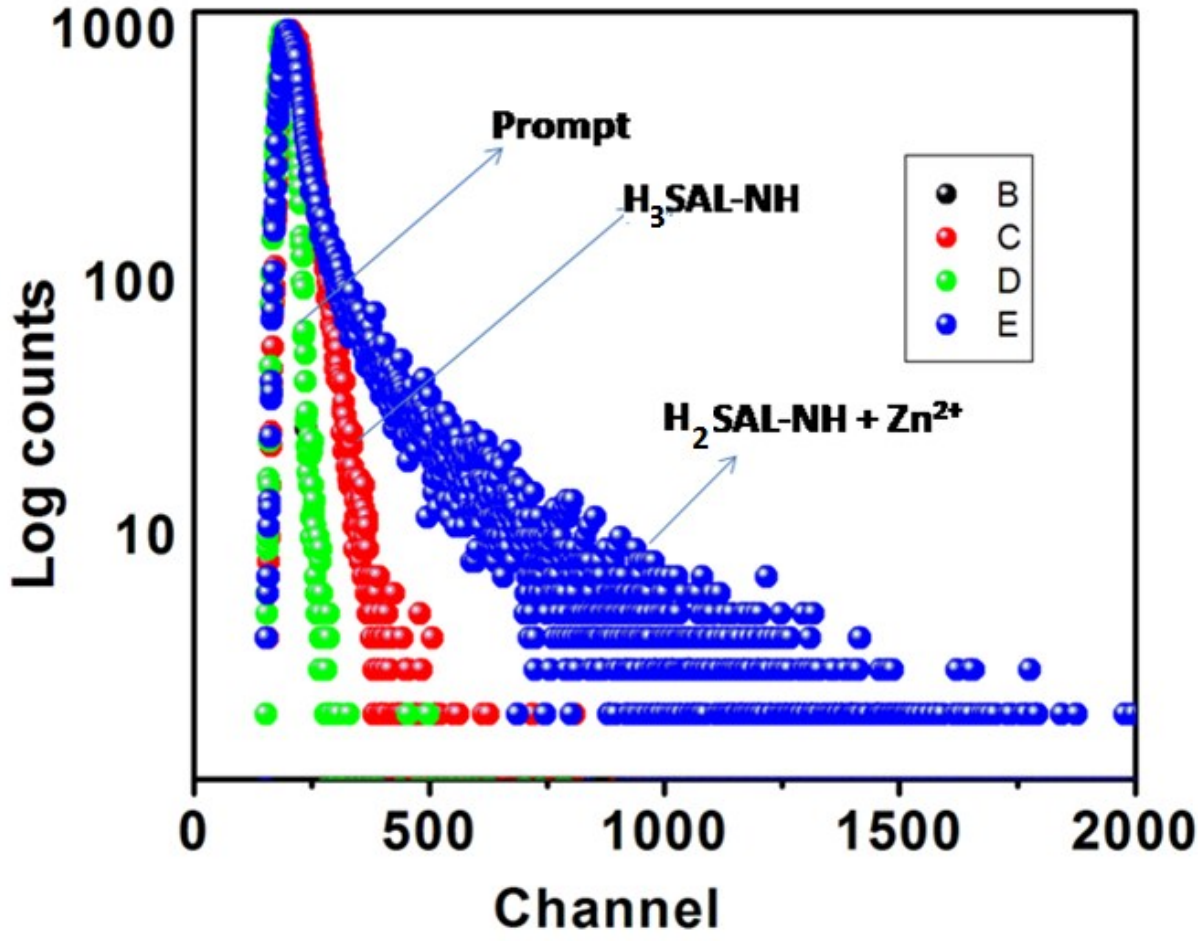

Figure S6. Lifetime plot of H_3SAL-NHand H_2SAL-NH + Zn^{2+} in T.H.F:H_2O(6:4 (V/V) in HEPES buffer.

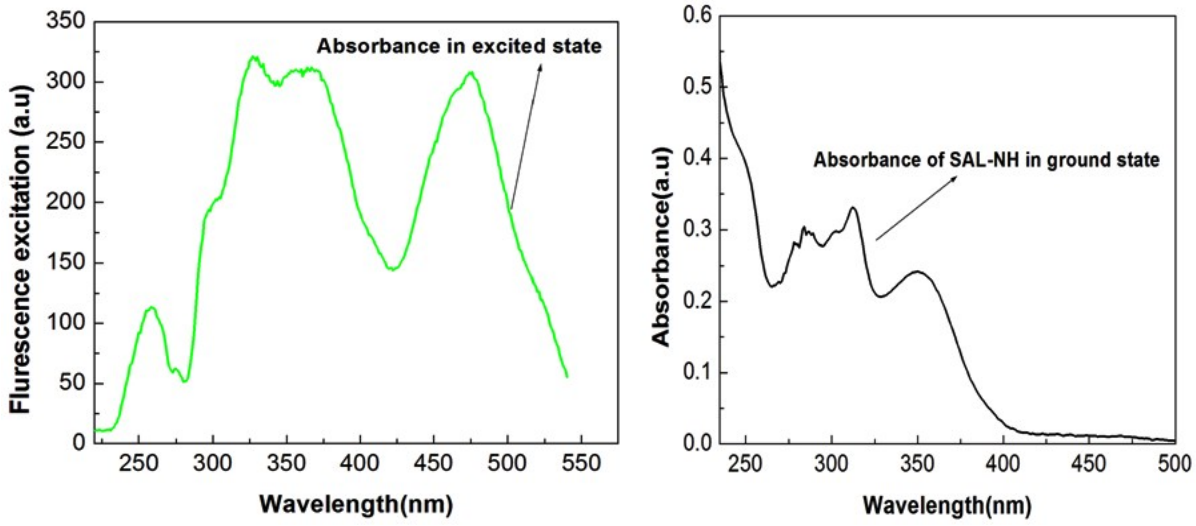

Figure S7 : UV-vis spectrum and Fluorescence excitation spectra of the ligand.

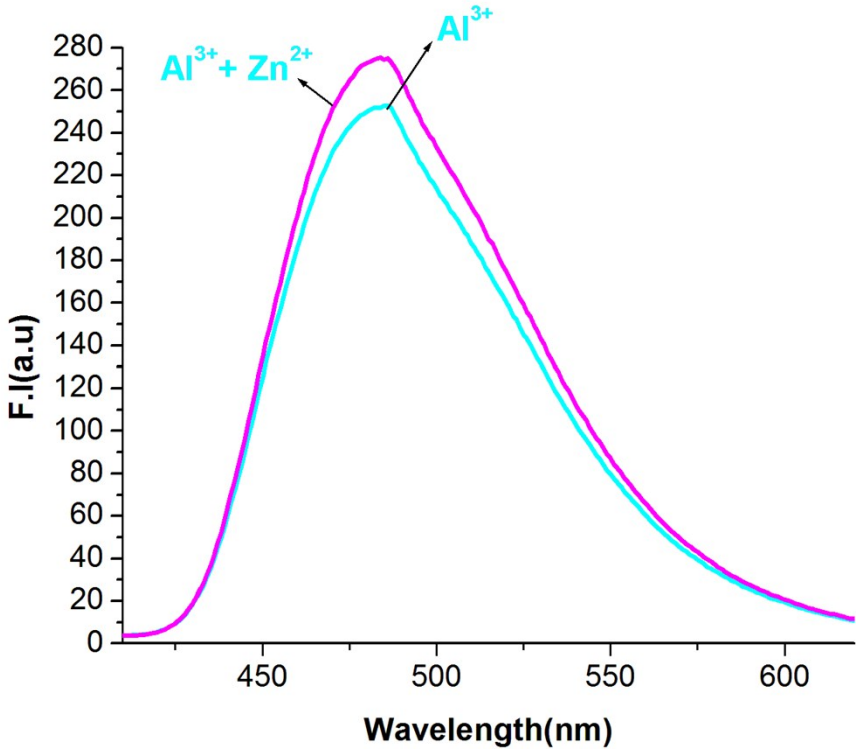

Figure S8. Spectra of Al^{3+}-SAL-NH and after the addition of 1 equivalent Zn^{2+}

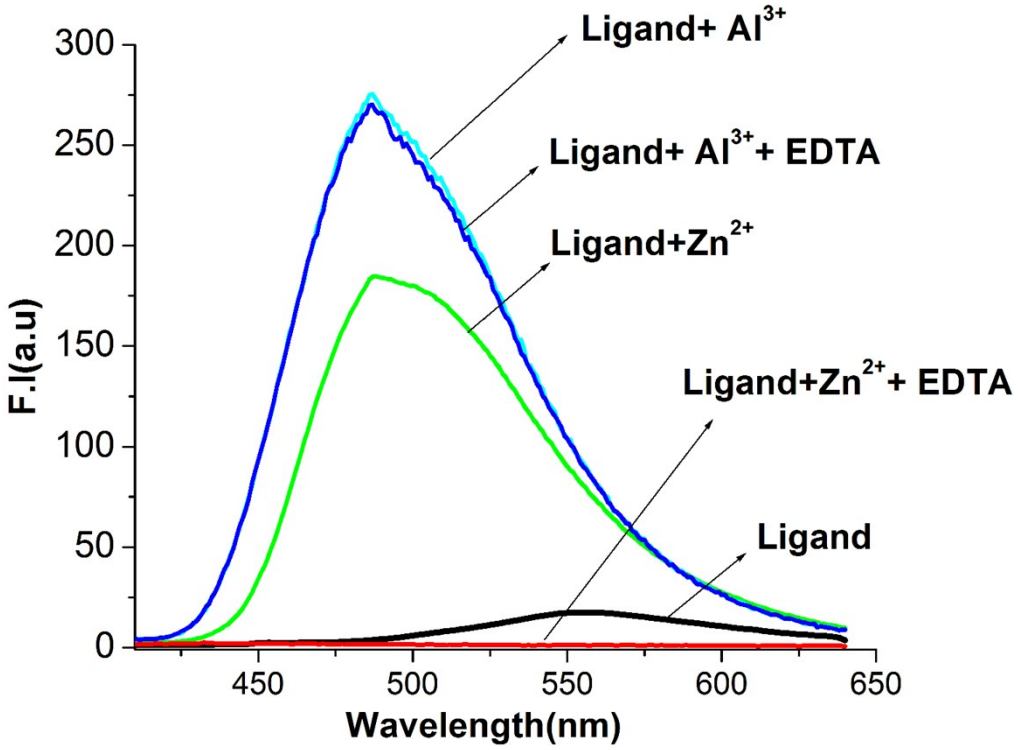

FigureS9. Reversibility plot of Zn^{2+} and Al^{3+}complex with Na_2H_2EDTA.

Calculation of the limit of detection (LOD):

The detection limit DL of **H_3SAL-NH**forM^{2+}(M = Zn and Al) was determined from3σ method by followingequation:**DL = K* Sb_1/S**

Where K = 2 or 3 (we take 3 in this case); Sb_1 is the standard deviation of the blank solution; S is the slope of thecalibration curve obtained from Linear dynamic plot of FI vs. [$\mathbf{M^{n+}}$].(n=2,3)

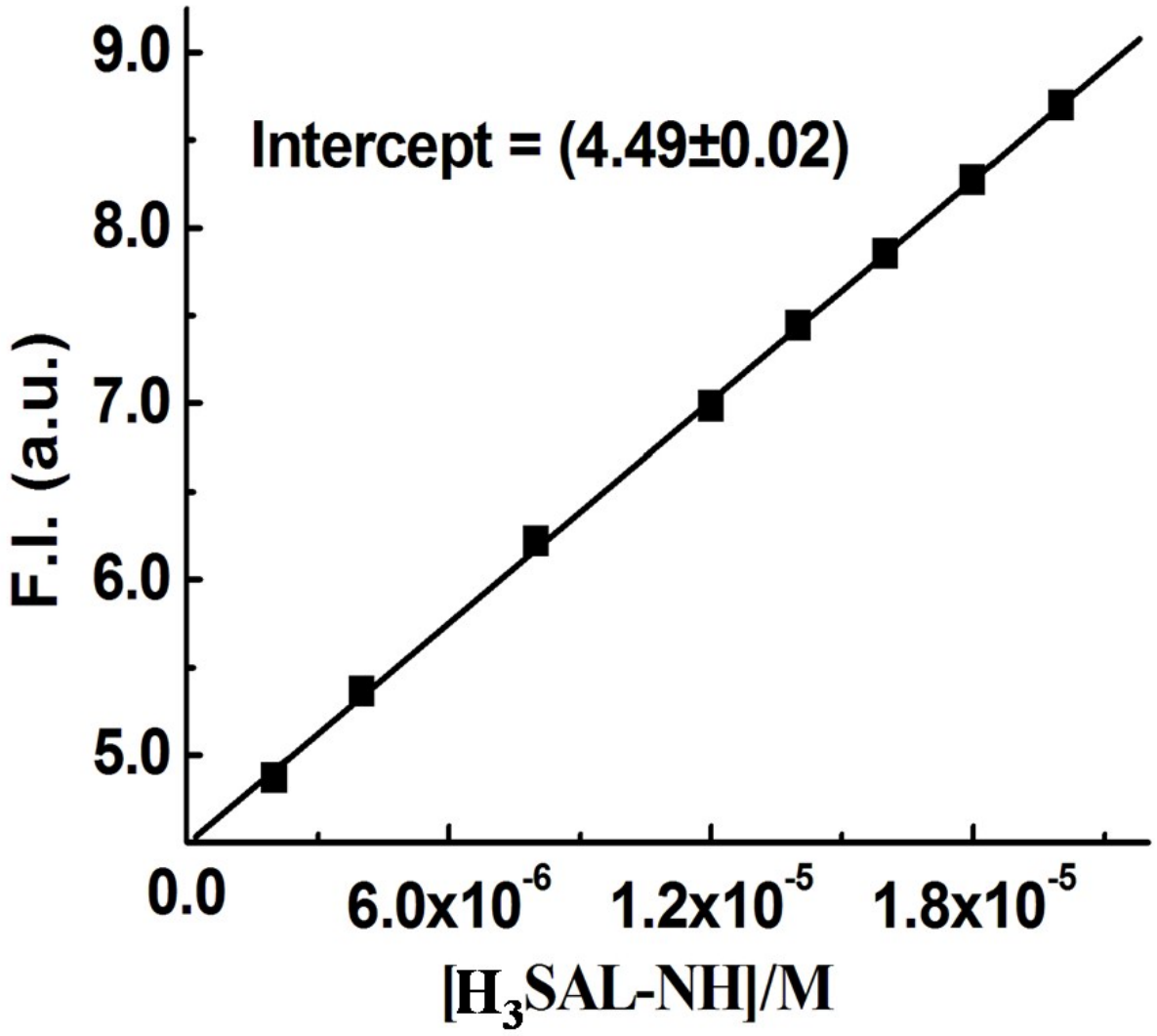

Figure S10. Determination of Sb_1 or the blank, H_3SAL-NH solution.

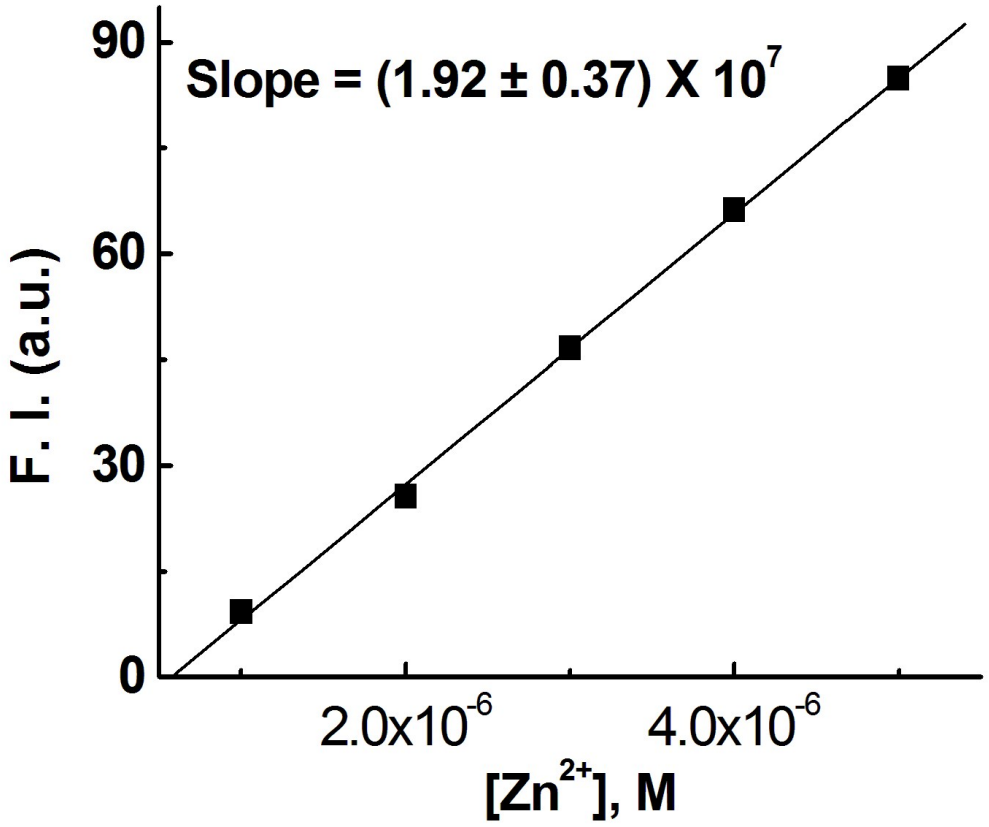

Figure S10a. Linear dynamic plot of FI at 496 nm vs. $[Zn^{2+}]$ for the determination of S (slope); $[H_3SAL\text{-}NH]$ =20 μM

LOD (Zn^{2+}) = (3 x 0.02)/1.92 x 10^7= 3.1nM

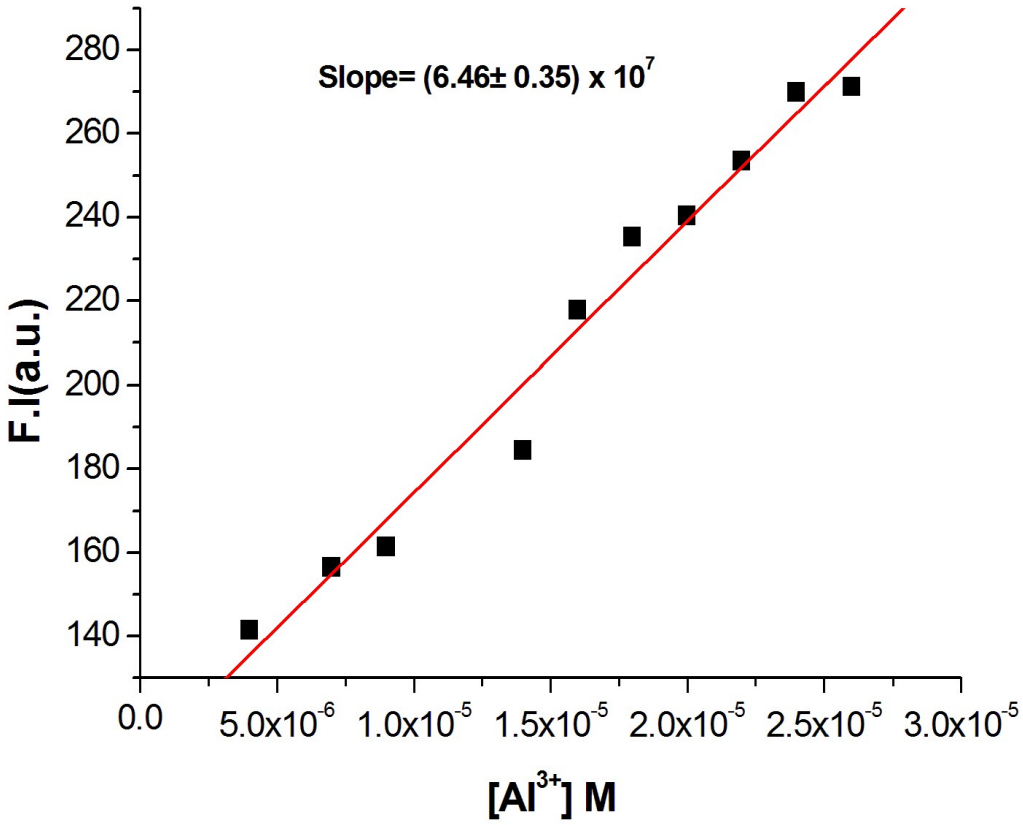

Figure S10b. Linear dynamic plot of FI at 486 nm vs. $[Al^{3+}]$ for the determination of S (slope); $[H_3SAL\text{-}NH]$ =20 µM

LOD (Al^{3+}) = (3 x 0.02)/6.46x 10^7 = 0.92 nM

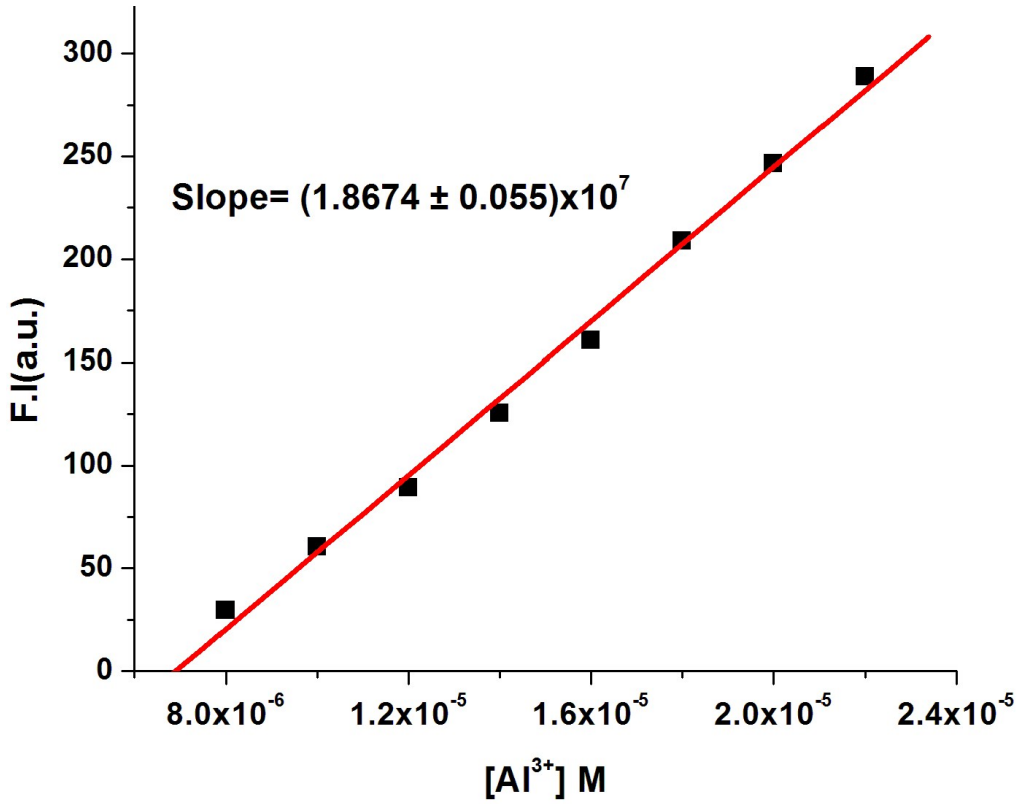

Figure S10c. Linear dynamic plot of FI at 486 nm vs. $[Al^{3+}]$ for the determination of S (slope); $[H_3SAL\text{-}NH]$ =20 µM, $[Na_2H_2EDTA]$ =20 µM, $[Zn^{2+}]$ =20 µM.

LOD (Al^{3+}) = (3 x 0.02)/1.86x 10^7 = 3.2 nM

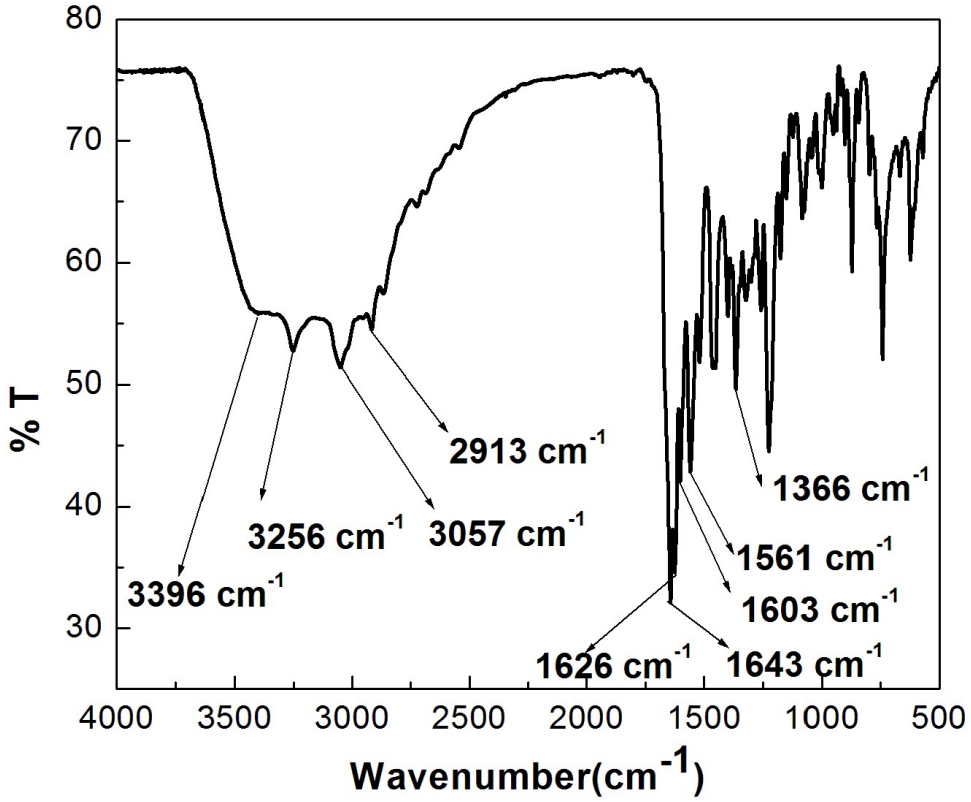

Figure S11. FT-IR spectrum of H_3SAL-NHin KBr pellet.

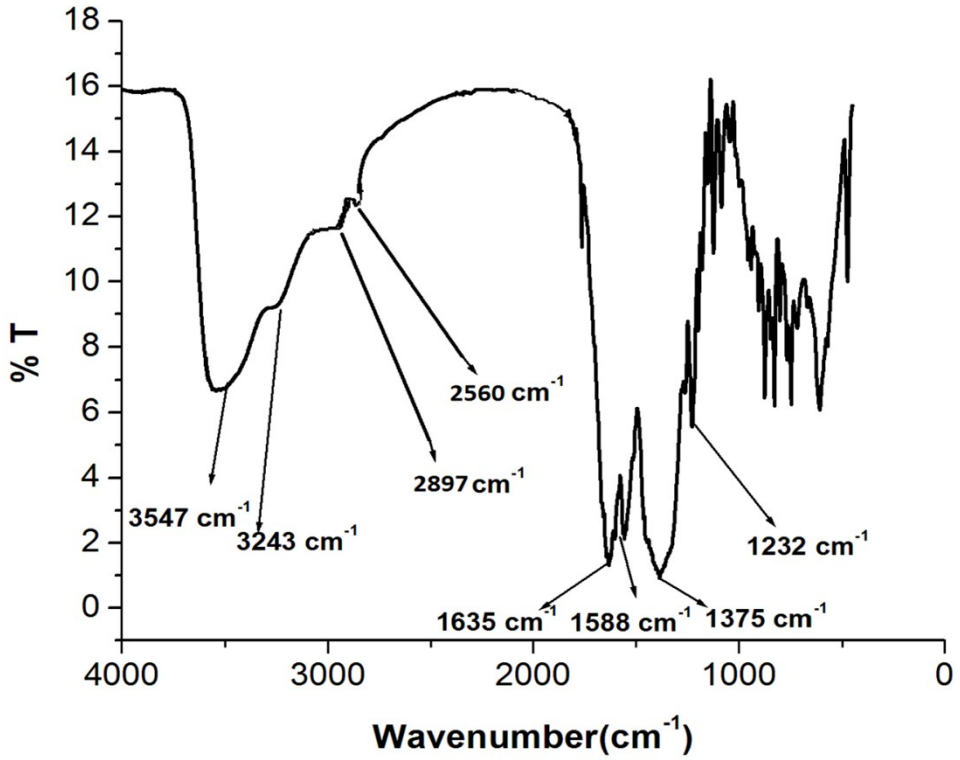

Figure S11a. FT-IR spectrum of complex **1** in KBr pellet.

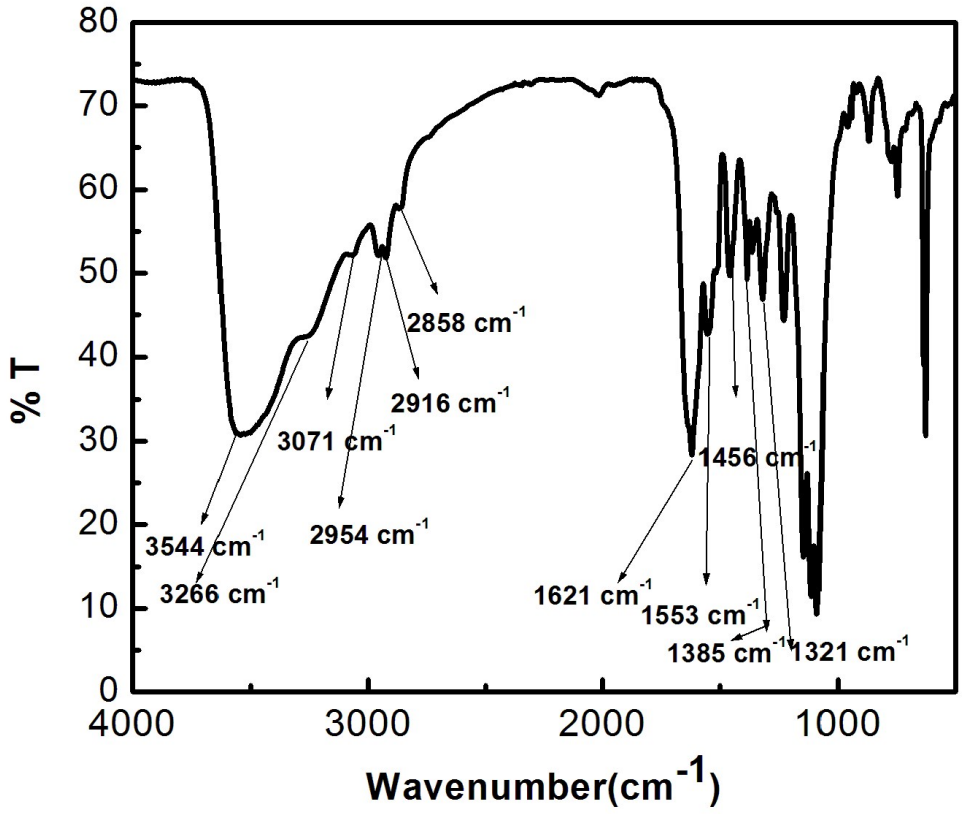

Figure S11b. FT-IR spectrum of complex **2** in KBr pellet.

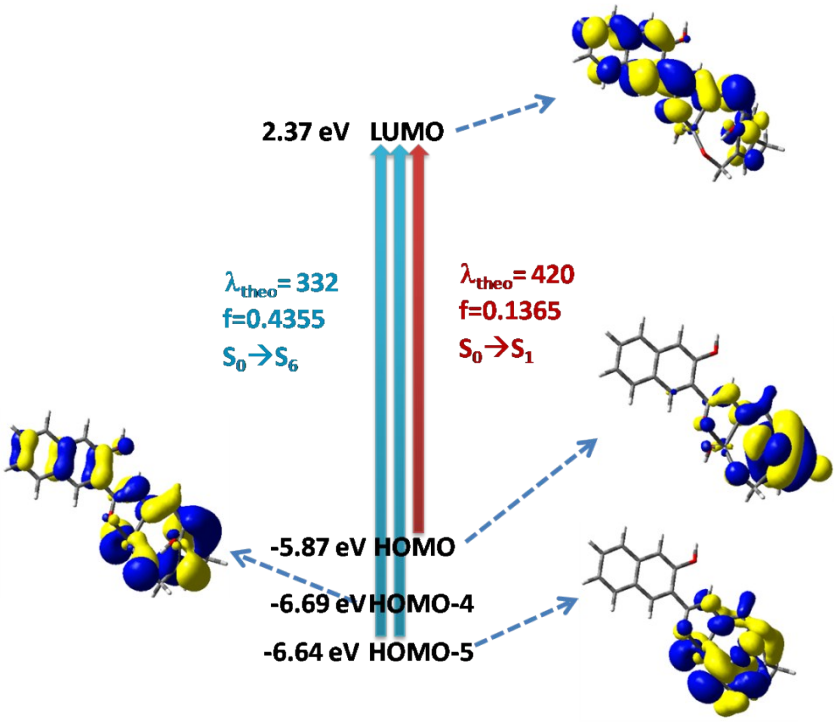

Figure S12. Frontier molecular orbitals involved in the UV-Vis absorption of the Zn-H_2SAL-NH complex in THF solutions.

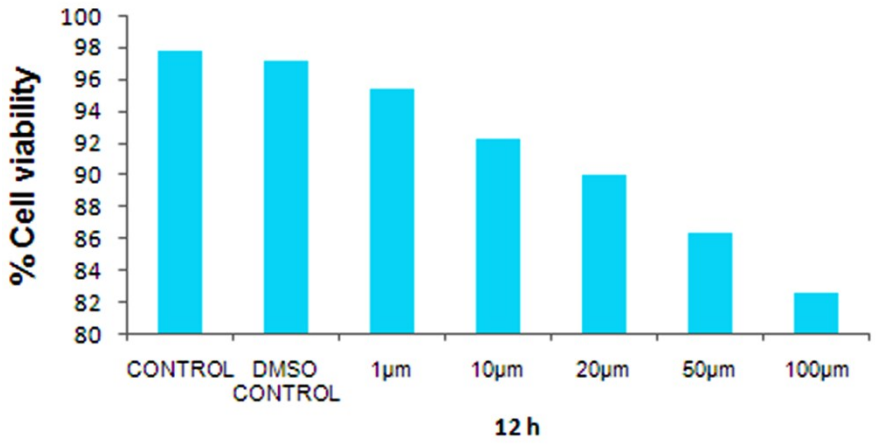

Figure S13.% cell viability of HepG2 cells treated with different concentrations (1 µM-100 µM) of H_3SAL-NH for 12 hour determined by MTT assay. Results were expressed as mean of three independent experiments.

Quantum Yield Determination:

Fluorescence quantum yields (Φ) were estimated by integrating the area under the fluorescence curves with the equation: $\Phi_{sample} = \frac{OD_{std}}{OD_{sample}} \times \frac{A_{sample}}{A_{std}} \times \Phi_{std}$

where, A was the area under the fluorescence spectral curve, OD was optical density of the compound at the excitation wavelength and η was the refractive indices of the solvent. Coumarine 153 was used as quantum yield standard (quantum yield is 0.54 in water)for measuring the quantum yields of H_3SAL-NHand [SAL-NH-Al^{3+}] and [H_2SAL-NH-Zn^{2+}] systems.

Table S1. ^{1}H-NMR chemical shifts in ppm of selected H-atoms in DMSO-d_6.

Compound	NH(d)	CH=N(c)	e	-CH_2(O)	-CH_2OH(m)	-OH(k)	-OH(j)
H_3SAL-NH	12.20	8.57(slightly increases)	8.44	5.08	4.56	11.03	11.62
SAL-NH – Al^{3+} (1)	12.20	8.58	8.44	5.08	4.23	(vanishes)	…….
H_2SAL-NH - Zn^{2+} (2)	12.20(No change)	8.61	8.45(almost unchanged)	5.08	4.24	11.04(broadening)	11.62

Table S2a: Selective bond distance and bond angles of H_3SAL-NH.

Bond distance(Å)		Bond angles(°)	
N22-N21	1.376	N21 C19 O20	123.21
C19-O20	1.249	C14 C19 O20	120.41
C24-N22	1.298	C25 C24 N22	120.73
C15-O17	1.402	C14 C15 O17	117.85
C27-O42	1.387	C25 C26 C28	121.17

Table S2b: Selective bond distance and bond angles of SAL-NH–Al^{3+} complex(1).

Bond distance(Å)		Bond angles(°)	
Al25-O30	1.998	N4 Al25 O22	130.64
Al25-O22	1.815	O22 Al25 O23	91.48
Al25-O23	1.856	N4 Al25 O48	95.60
Al25-N4	2.107	N4 Al25 O30	89.96
Al25-O48	1.806	O22 Al25 O48	132.15
-------	---------	O23 Al25 O48	109.63
--------	--------	O23 Al25 O30	167.31
-------	--------	O30 Al25 O48	80.16

Table S2c: Selective bond distance and bond angles of H_2SAL-NH–Zn^{2+} complex(2).

Bond distance(Å)		Bond angles(°)	
Zn44-O45	1.841	O40 Zn44 O45	129.87
Zn44-O20	2.128	N22 Zn44 O45	100.42
Zn44-O40	1.956	N22 Zn44 O40	119.66
Zn44-N22	2.247	O20 Zn44 O45	104.33
		O20 Zn44 O40	114.58

Table S3. Selected parameters for the vertical excitation (UV-VIS absorptions) of **H_3SAL-NH**; electronicexcitation energies (eV) and oscillator strength (f), configurations of the low-lying excited states of L; calculation of the $S_0 \rightarrow S_n$ energy gaps on optimized ground- state geometries (UV-vis absorption).

Electronic transition	Composition	Excitation energy	Oscillator strength (*f*)	CI	Assign	λ_{exp} (nm)
$S_0 \rightarrow S_4$	HOMO → LUMO	3.46eV (357 nm)	**0.7285**	0.69765	ILCT	350
$S_0 \rightarrow S_{11}$	HOMO – 2 → LUMO	3.9850 eV (311nm)	**0.1418**	0.63613	ILCT	313
	HOMO → LUMO + 1			0.23905	ILCT	
$S_0 \rightarrow S_{12}$	HOMO – 4 → LUMO	4.1734eV(297 nm)	**0.4127**	0.17226	ILCT	303
	HOMO – 3 → LUMO			0.17041	ILCT	
	HOMO – 2 → LUMO			----	ILCT	
	HOMO → LUMO+1			0.60798	ILCT	

Table S4. Main calculated optical transition for the complex 1 with composition in terms of molecular orbital contribution of the transition, vertical excitation energies, and oscillator strength in THF

Electronic transition	Composition	Excitation energy	Oscillator strength (*f*)	CI	Assign	λ_{exp} (nm)
$S_0 \rightarrow S_2$	HOMO-1 → LUMO	3.1024eV (399 nm)	**0.0565**	0.53202	MLCT/ILCT	398
	HOMO→LUMO			0.42889		
	HOMO → LUMO + 1			------		
$S_0 \rightarrow S_5$	HOMO – 4 → LUMO	3.6303 eV (341nm)	**0.0401**	----	MLCT/ILCT	335
	HOMO-2 → LUMO			0.59678	MLCT/ILCT	
	HOMO-2 → LUMO+1			0.19833	MLCT/ILCT	
$S_0 \rightarrow S_6$	HOMO – 4 → LUMO	3.9416eV(314 nm)	**0.2680**	-----	MLCT/ILCT	321
	HOMO – 3 → LUMO			0.57959	MLCT/ILCT	
	HOMO – 2 → LUMO+1			----	MLCT/ILCT	

Table S5 Main calculated optical transition for the complex 2 with composition in terms of molecular orbital contribution of the transition, vertical excitation energies, and oscillator strength in THF

Electronic transition	Composition	Excitation energy	Oscillator strength (*f*)	CI	Assign	λ_{exp} (nm)
$S_0 \rightarrow S_1$	HOMO → LUMO	2.9490eV (420nm)	0.1365	0.69534	MLCT/ILCT	412
	HOMO → LUMO + 1			----		
$S_0 \rightarrow S_6$	HOMO – 5 → LUMO	3.7267 eV (332nm)	0.4355	----	MLCT/ILCT	335
	HOMO-4 → LUMO			0.58118	MLCT/ILCT	

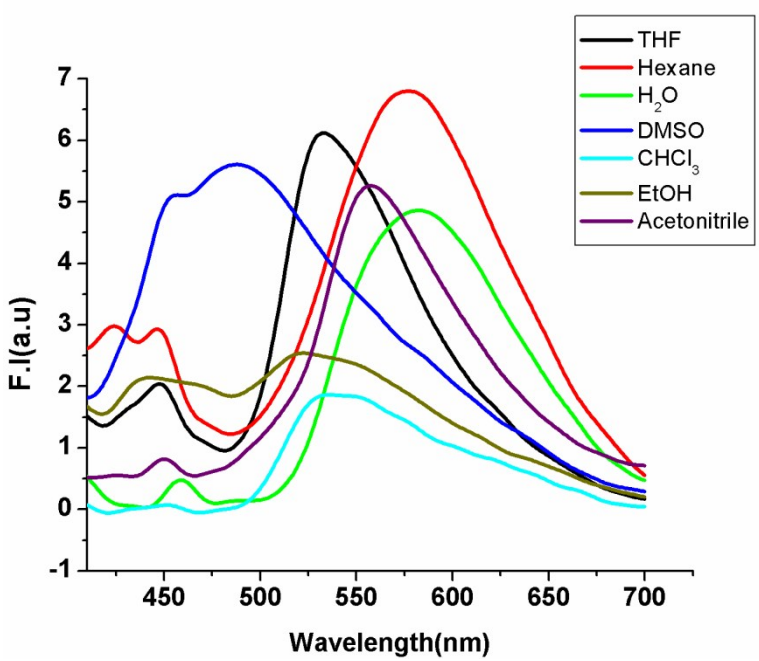

Figure S14. Emission band at lower wavelength (around 430nm) and at higher wavelength(above 520nm) in various solvents.

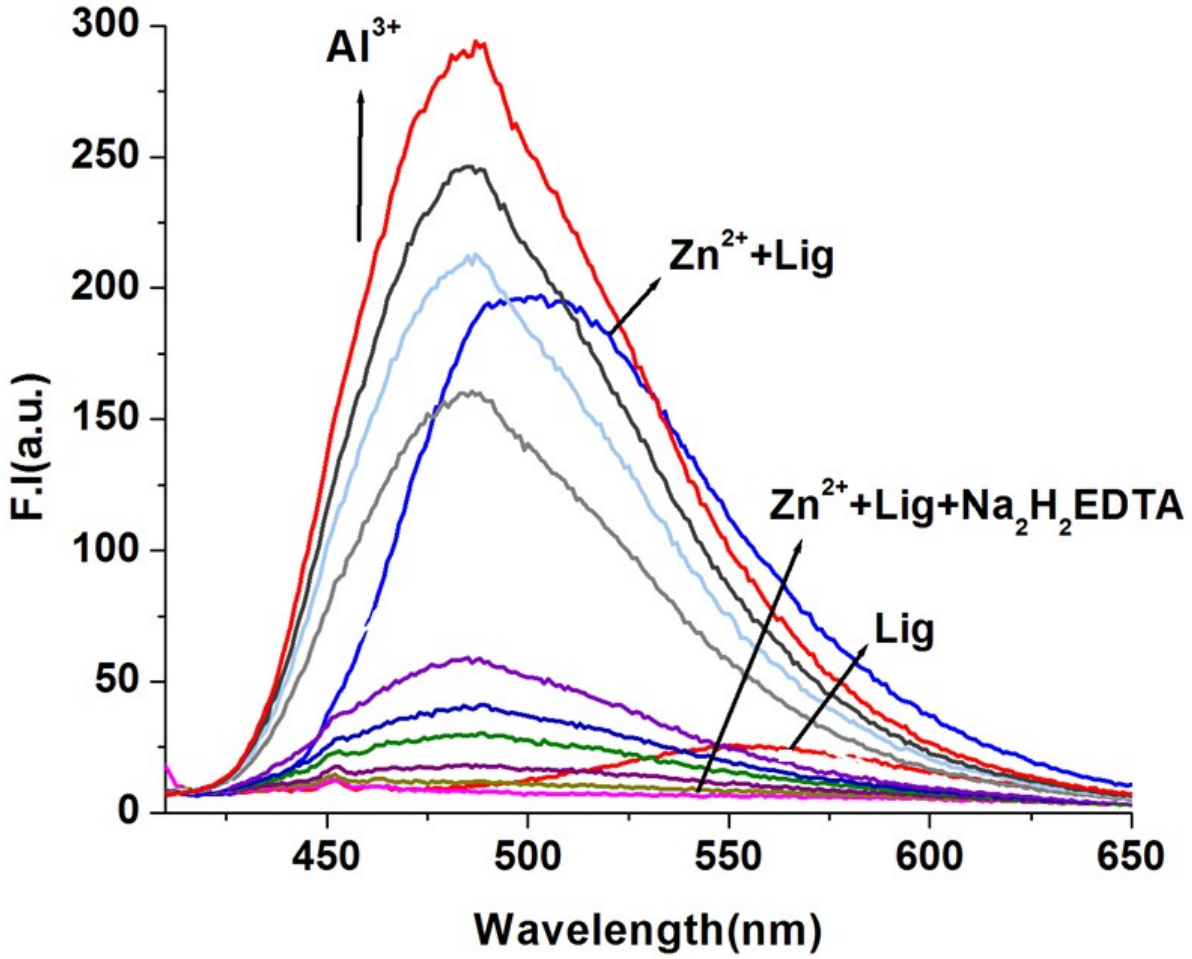

Figure S15. Titration with Al^{3+} in presence of 1equivalent H_2SAL-NH—Zn^{2+} and 1 equivalent Na_2H_2EDTA.